

# Quantitative invalidation characterization of Portland cement based on BSE and EDS analysis



Shengxing Wu<sup>a</sup>, Kewei Sun<sup>a</sup>, Haitao Zhao<sup>a,b,\*</sup>, Fengchen Zhang<sup>c</sup>

<sup>a</sup> College of Civil and Transportation Engineering, Hohai University, Nanjing 210098, PR China

<sup>b</sup> State Key Laboratory for GeoMechanics and Deep Underground Engineering, China University of Mining & Technology, Xuzhou 221116, PR China

<sup>c</sup> College of Mechanics and Materials, Hohai University, Nanjing 210098, PR China

## HIGHLIGHTS

- A quantitative invalidation characterization method of Portland cement is established.
- Crystal structures with lengths greater than 3.0 μm appear around cement particles can be regarded as complete invalidation.
- The relationship between the content of oxide containing Al and the degree of invalidation of Portland cement is proposed.

## ARTICLE INFO

### Article history:

Received 7 June 2017

Received in revised form 26 September 2017

Accepted 27 September 2017

### Keywords:

Portland cement

Invalidation

Characterization

BSE

EDS

Oxide containing aluminium

## ABSTRACT

The degradation of mechanical properties of Portland cement caused by the invalidation of Portland cement is a serious problem that affects the quality of concrete nowadays. However, an effective invalidation characterization method of Portland cement has not been set up. Back scattering electron (BSE) and energy-dispersive spectrometry (EDS) were adopted to quantitatively characterize the invalidation of Portland cement in this study. The EDS results demonstrated that the acicular crystals generated near cement particles in BSE images are ettringites. Therefore the invalidation of Portland cement is mainly caused by the expansive ettringite generated from the hydration of oxides containing Aluminium, and crystallisation corrosion is the main invalidation mechanism. When the microstructure of acicular morphology with a length longer than 3.0 μm is observed from BSE images of Portland cement samples, the cement can be quantified as exhibiting complete invalidation. Meanwhile, the content changing of element in the area of ettringite formation acquired with EDS analysis can also be used to characterize the invalidation of Portland cement. When the content of oxide containing aluminium is not more than 5.0%, the cement is not judged as invalidated; the invalidation of cement will occur once the content of oxide containing aluminium exceeded 5.0%; when the content of oxide containing aluminium exceeded 10.0%, the cement is considered completely invalidated.

© 2017 Elsevier Ltd. All rights reserved.

## 1. Introduction

The quality of Portland cement significantly influences the performance of concrete [1–3]. Existing standards do not specify the shelf life of Portland cement. However, invalidation of Portland cement is likely to occur due to the influence of environmental conditions. While the compressive strength of Portland cement is 5 MPa lower than the standard compressive strength, mechanical performance of cement will not be up to standard [4]. As a result, the compressive strength of concrete by using invalidated cement

cannot be guaranteed, and quality-related safety accidents could frequently occur [5–7]. Therefore, invalidation characterization of Portland cement is necessary.

In the research on the invalidation characterization of Portland cement, visual observation and strength test methods have been mainly used. The visual observation method is used to detect severe caking on cement surface according to a phenomenological empirical experience. Chen [8] classified agglomeration during cement storage classified into three categories: warehouse caking, pile caking and bag caking. Furthermore, they provided suggestions for preventing agglomeration of Portland cement by controlling the content of C<sub>3</sub>A in the clinker. However, no quantitative parameters of the corresponding relationship between the content of C<sub>3</sub>A and invalidation of Portland cement were presented. The

\* Corresponding author at: College of Civil and Transportation Engineering, Hohai University, Nanjing 210098, PR China (H. Zhao).

E-mail address: [zhaoh@hhu.edu.cn](mailto:zhaoh@hhu.edu.cn) (H. Zhao).

compressive strength test method is used to determine cement invalidation by testing the compressive strength of 28-day cement mortar specimens and examining whether the strength of the cement meets the specifications. However, this method exhibits strong hysteresis. Zou [9] utilised energy-dispersive spectrometry (EDS) to determine the types and contents of elements in mineral constituents in montmorillonite powder to determine which varieties of montmorillonite drugs fail. He [10] utilised scanning electron microscopy (SEM), EDS and X-ray diffraction to analyse and characterize the corrosion invalidation products on the steel structures of a substation. The results showed that the corrosion invalidation of steel structures was caused by the electrochemical corrosion of carbon steel in humid atmosphere. Inspired by the above two research in different fields and so on, we think that the microscopic detection is very useful for the quantitative invalidation characterization of Portland Cement. Therefore, a quick and accurate method of quantitative invalidation characterization of Portland cement was proposed in this study by using microscopic analysis methods, such as BSE and EDS, to investigate the microstructure's morphological change and the invalidation essence of Portland cement.

## 2. Materials and methods

### 2.1. Materials

In this experiment, P-II 52.5 Portland cement produced by Jiangnan-Onoda Company (Nanjing, China) was used. Physical properties and chemical composition of the Portland cement are shown in Tables 1 and 2, respectively. One kind of fine sand for making cement mortar was standard quartz sand. The kind of sand were used as aggregate, i.e., fine sand with 98% SiO<sub>2</sub> and an apparent density of 2640 kg/m<sup>3</sup>, a fineness modulus of 1.8 and a maximum diameter of 2.35 mm. Cement mortar moulds (40 mm × 40 mm × 160 mm), a constant-temperature curing box and a low-speed cutting machine were utilised for the experiments. The materials used for cement micro-sample preparation included sandpaper, diamond paste, clean wiper, anhydrous ethanol and silastic moulds.

### 2.2. Experimental method

#### 2.2.1. Sample preparation

The main factors that affect the invalidation of Portland cement are humidity and storage period. Therefore, the cement invalidation simulation test mainly investigated the effect of relative humidity and age on the invalidation of Portland cement. The invalidation process of Portland cement under three different humidity conditions, i.e. 75.0%, 85.0% and 95.0, was tested in three humidity environments. Considering the advantages of saturated solutions, such as favourable chemical stability, small temperature coefficient, weak volatility and low toxicity, Organisation Internationale de Metrologie Legale selected 11 types of saturated salt solutions to form a salt solution standard relative humidity table [11]. In this experiment, three types of cheap and commonly available salt, namely, sodium chloride (NaCl), potassium chloride (KCl) and potassium sulphate (K<sub>2</sub>SO<sub>4</sub>) (as shown in Table 3) were selected to compound the corresponding saturated saline solutions. The humidity source was formed of the constant relative humidity (humidity fixed point) which was maintained in a confined space above the saturated saline solution. At room temperature of 25.0 °C, the saline solutions of the three relative humidity levels were compounded in glass bottles as salt cellars. The cement was stored above the salt solution for 7, 14, 30 and 90 day in a closed environment to observe the invalidation process. The design of the sample preparation is shown in Table 4. The sample cured for 7 day in an environment with a relative humidity of approximately 75.3% was labelled as A7. The other samples were labelled as A14, A30, A90, B7, B14, B30, B90, C7, C14, C30 and C90. Twelve groups of samples from A7 to C90 were tested. Appropriate amounts of cement were obtained from each group to prepare microscopic cement samples with different ages for SEM/EDS detection. Each group was subjected to a mortar compression test.

**Table 1**  
Physical properties of Portland cement.

Test projects	Specific surface area (m <sup>2</sup> /kg)	Water demand of normal consistency (%)	Initial setting (min)	Final setting (min)	Stability
Measured value	373.0	27.9	174.0	229.0	Qualified

#### 2.2.2. SEM/EDS experiment

A SEM/EDS experiment was conducted to determine the microscopic morphologies of the cement samples under different humidity environments and ages. Because different laboratories will have different scanning electron microscopy (SEM) equipment, only generalities can be presented in this portion of the documentation. Beginning with material preparation, the cement powder of samples approximately 25 g are mixed with a low viscosity epoxy resin to form an almost dry paste [12]. The epoxy is subsequently cured at 80 °C for 12 h and the specimen was then cut into 1 cm<sup>3</sup> cubes with the cutting machine, ground and polished to achieve 7 mm-thick samples with parallel surfaces. The samples were washed with absolute ethyl alcohol and utilised in the SEM/EDS experiment. SEM was used to observe the change of microstructure morphology near the cement particles. In the meanwhile, EDS was used to detect the contents of mainly existing elements distributed in a certain range of the area which indicated microstructure changes in SEM image. In addition, the contents of elements were equivalently converted to the corresponding oxides in the results of EDS, and the corresponding oxides are major oxide composition of Portland cement. For viewing cement samples, typical settings are an accelerating voltage of 12 kV of and probe currents of 2 nA and 10 nA for the backscattered electron and X-ray imaging, respectively.

#### 2.2.3. Compressive strength test

The cement stored for certain periods under each humidity condition were mixed with sand and water at certain proportions and then moulded [13]. Cement mortar specimens were prepared with cement to-sand ratio of 1:3 and water to-binder ratio of 0.5. Six samples (40 mm × 40 mm × 160 mm) were moulded in each batch. The cement mortar specimens were demoulded after 24 h and maintained in a standard curing room. The curing temperature was 20 ± 1 °C, the relative humidity was maintained at 95% and the curing period was 28 day. Compressive strength tests were performed on a pressure tester at a loading rate of 1.5 kN/s.

## 3. Results and discussion

### 3.1. SEM/EDS results

After the cement samples were stored for 7d above the closed NaCl, KCl and K<sub>2</sub>SO<sub>4</sub> solutions, the surfaces of the cement samples did not cake. The BSE images are shown from Figs. 1–3. No suspected needle crystals appeared near complete particles. X-ray energy spectrum analysis was conducted to determine the contents of oxides corresponding to the BSE image areas, as shown in Table 5. The contents of oxides containing Al in A7, B7 and C7 were 3.3%, 3.5% and 3.2%, respectively, which did not exceed 5.0%.

After the cement samples were stored for 14 day above the closed NaCl solution, the surfaces of the cement samples did not change. The colour of cement powder deepened slightly after being stored for 14 day above the closed KCl solution.

After the cement samples were stored above the closed K<sub>2</sub>SO<sub>4</sub> solution for 14 day, the colour of the cement powder surface deepened significantly, and the cement powder exhibited slight agglomeration. The BSE images of the samples stored for 14 day in the same SEM/EDS operation are shown from Figs. 4–6. Needle crystals with lengths of approximately 1.0 μm appeared, as shown in Figs. 5 and 6. However, the needle structures had a narrow distribution range. Furthermore, X-ray energy spectrum analysis was conducted to determine the contents of oxides containing Al and K (as shown in Table 5). The contents of oxides containing Al in A14, B14 and C14 were 4.9%, 6.9% and 8.1%, respectively, which do not exceed 10.0%.

After the cement samples were stored above the closed NaCl solution for 30 d, the colour of the cement powder deepened slightly. The hardness of the cement powder increased, and slight agglomeration was observed after the cement samples were stored above the closed KCl solution for 30 day. After being stored above the closed K<sub>2</sub>SO<sub>4</sub> solution for 30 d, the cement powder caked

**Table 2**  
Chemical composition of Portland cement (%).

Oxide	CaO	SiO <sub>2</sub>	Al <sub>2</sub> O <sub>3</sub>	Fe <sub>2</sub> O <sub>3</sub>	S <sub>2</sub> O <sub>3</sub>	MgO	K <sub>2</sub> O	NaO
Contents	63.81	19.52	4.11	2.89	1.25	3.25	0.13	0.64

**Table 3**  
Equilibrium relative humidity of selected saturated salt solution (%).

Temperature (°C)	NaCl	KCl	K <sub>2</sub> SO <sub>4</sub>	Distilled water
25.0	75.3 ± 0.2	84.3 ± 0.3	97.3 ± 0.5	100.0

**Table 4**  
Schemes of the sample preparation.

Relative humidity (%)	Age (d)			
	7	14	30	90
75.3 ± 0.2	A7	A14	A30	A90
84.3 ± 0.3	B7	B14	B30	B90
97.3 ± 0.5	C7	C14	C30	C90

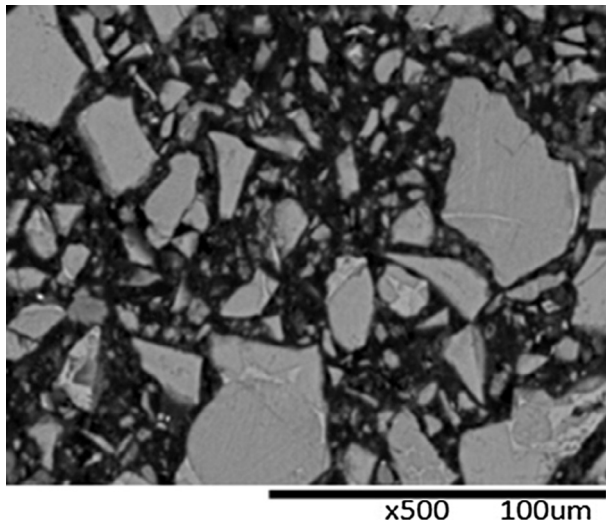


**Fig. 1.** BSE image of A7.

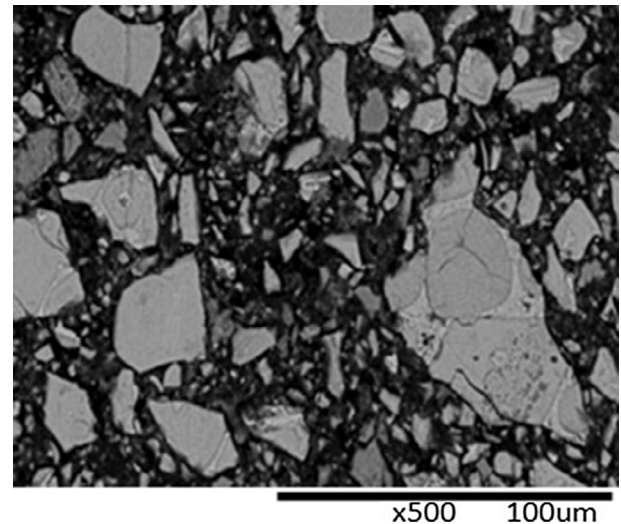


**Fig. 3.** BSE image of C7.

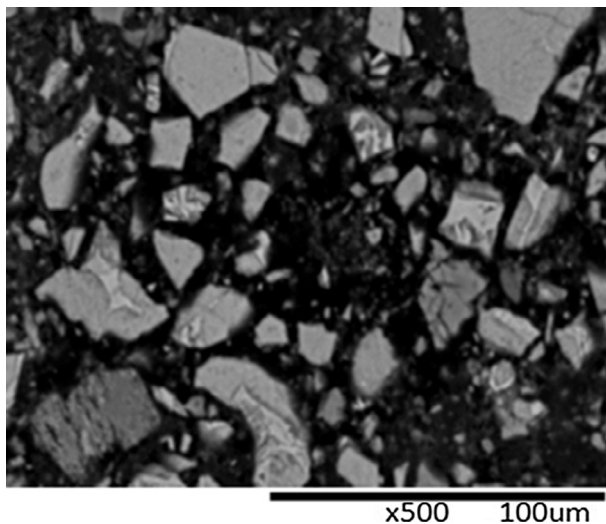


**Fig. 2.** BSE image of B7.

severely. The BSE images of the samples stored for 30 d in the same SEM/EDS operation are shown from Figs. 7–9. Needle crystals with lengths of approximately 1.0 µm appeared, as shown in Fig. 7. Needle crystals with lengths of approximately 3.0 µm were evident in Figs. 8 and 9. X-ray energy spectrum analysis was also conducted to determine the contents of oxides containing Al and K (as shown in Table 5). The contents of oxides containing Al in A30, B30 and C30 were 12.6%, 15.7% and 19.7% respectively, all of which exceed 10.0%.

After the cement samples were stored for 90d above the closed NaCl, KCl and K<sub>2</sub>SO<sub>4</sub> solutions, the colour of the cement sample surfaces deepened slightly, and the cement samples caked severely. The cement powder could not be restored with knocking the cement samples. The BSE images of the samples stored for 90 d in the same SEM/EDS operation are shown from Figs. 10–12. Needle crystals with lengths of approximately 5.0 µm appeared, as shown in all three images. The needle crystals were similar to those observed in the images of the samples cured for 30 d. However, the lengths and areas of the crystals increased. The local region presented a dense network. X-ray energy spectrum analysis was again conducted to determine

**Table 5**  
EDS results from SEM images in Figs. 1–12 (%).

Number of sample	Elemental oxides				
	Al <sub>2</sub> O <sub>3</sub>	SiO <sub>2</sub>	K <sub>2</sub> O	CaO	Total
A7	3.3	27.1	0.8	68.8	100.0
A14	4.9	25.7	1.0	68.4	100.0
A30	12.6	24.8	0.7	61.8	100.0
A90	15.5	21.5	0.6	62.4	100.0
B7	3.5	28.0	0.9	67.6	100.0
B14	6.9	24.9	1.2	67.0	100.0
B30	15.7	19.4	0.6	64.3	100.0
B90	17.7	19.4	0.6	62.3	100.0
C7	3.2	28.2	0.7	67.9	100.0
C14	8.1	23.9	1.5	66.5	100.0
C30	19.7	20.4	0.4	59.5	100.0
C90	21.4	20.3	0.4	57.9	100.0

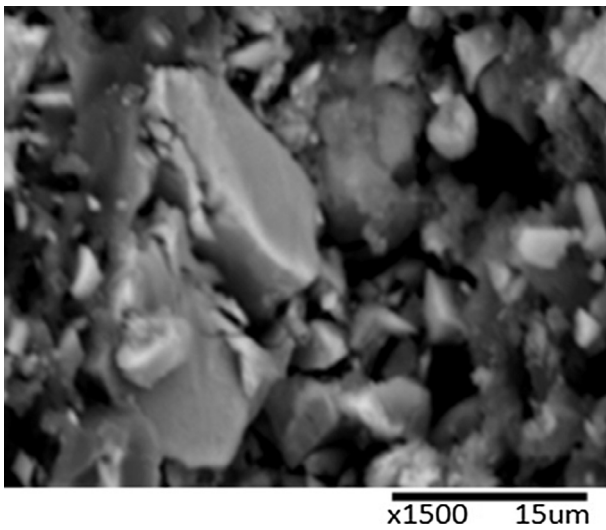


**Fig. 4.** BSE image of A14.

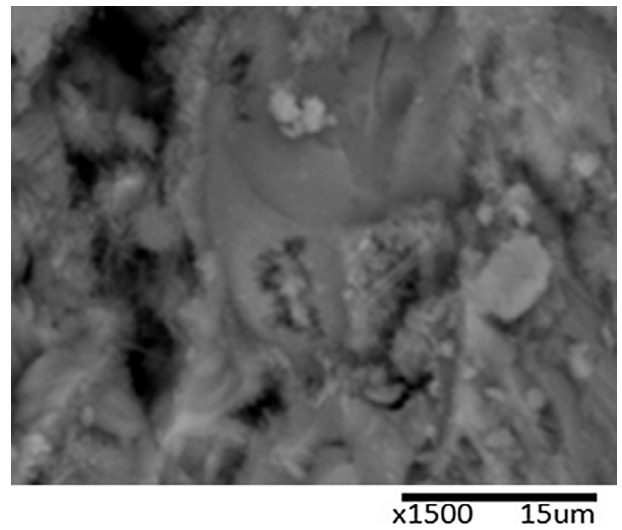


**Fig. 6.** BSE image of C14.

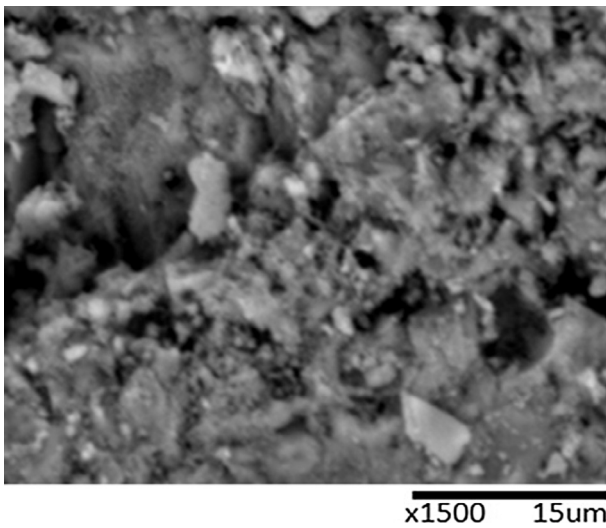


**Fig. 5.** BSE image of B14.

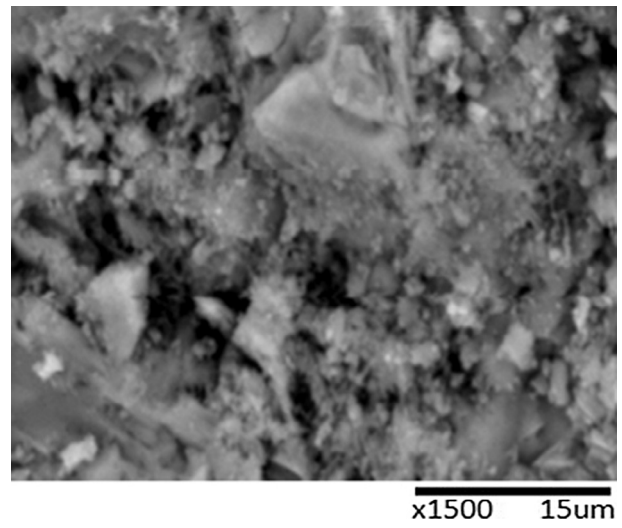


**Fig. 7.** BSE image of A30.

the contents of the oxides containing Al and K (as shown in Table 5). The contents of oxides containing Al in A90, B90 and C90 were 15.5%, 17.7% and 21.4%, respectively, all of which exceed 15.0%.

### 3.2. Invalidation mechanism and quantitative characterization

#### 3.2.1. Invalidation mechanism

Chen [8] observed cement clinkers with large contents of alkali, sulphate and C<sub>3</sub>A. There are two kinds of reactions that result in

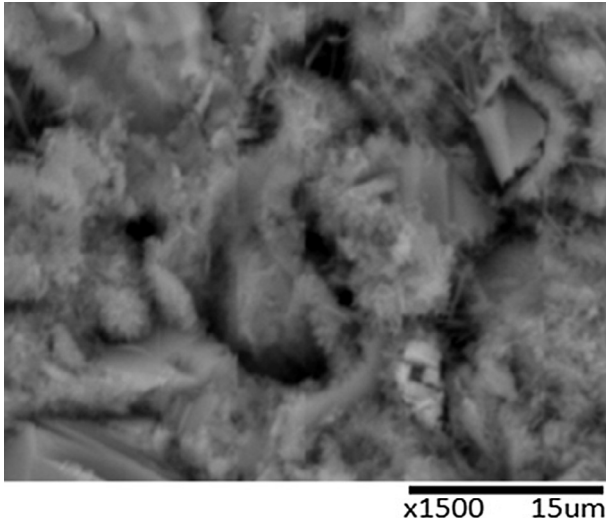


Fig. 8. BSE image of B30.

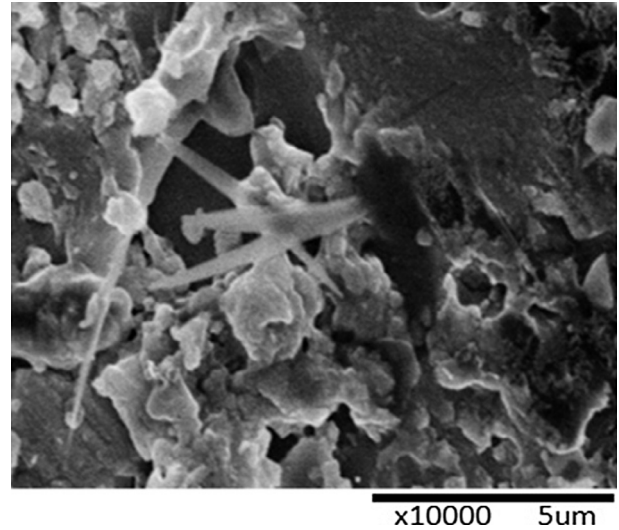


Fig. 11. BSE image of B90.

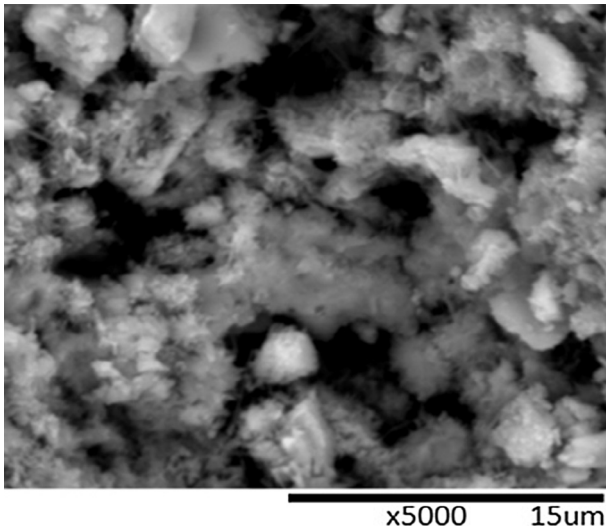


Fig. 9. BSE image of C30.

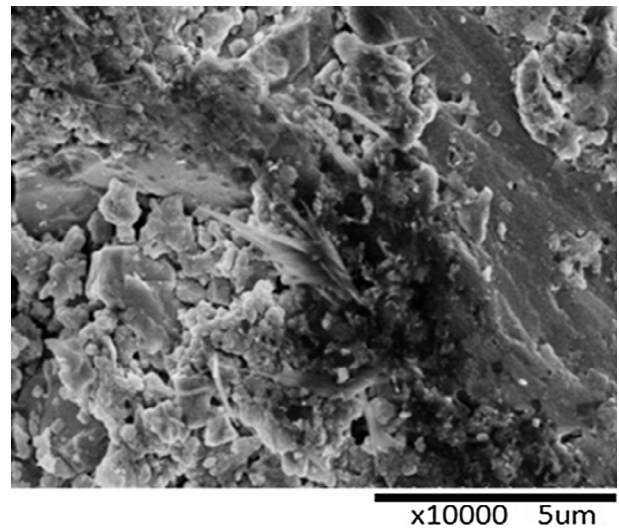


Fig. 12. BSE image of C90.

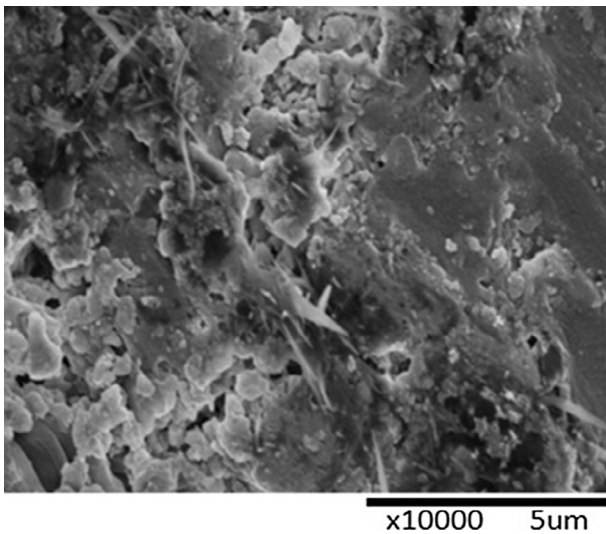
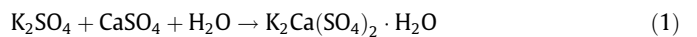
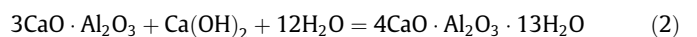


Fig. 10. BSE image of A90.

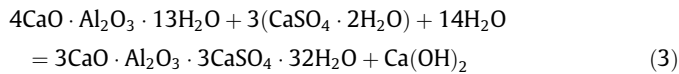
cement agglomeration. One reaction is potassium sulphate and calcium sulphate mixed with cement in the form of gypsum can react in the presence of water, and then the reaction product is hydrated potassium calcium sulphate.



In the other reaction, ettringite, which is considered cement bacillus, is likely to be generated in the reaction among CH, gypsum in cement and free water because of the strong activity of  $\text{C}_3\text{A}$  in clinker minerals. The process consumes excessive Ca ions and results in cementation decline and invalidation. Ettringite (Aft phase) is one of the important hydration products of cement; it accounts for approximately 7.0% of Portland cement hydration products after complete hydration. Many research have reported that the ettringite generated from hydration reaction of cement is as follows [14–16]:



The hexagonal tabular crystal  $\text{C}_4\text{AH}_{13}$  generated after hydration reacts with gypsum; as a result, ettringite is generated. The reaction equation is as follows:



Potassium gypsum and ettringite are columnar or acicular structures [17]. The formation of these two expandable crystals consumes cement mineral components and results in the loss of the cementitious component in cement. Meanwhile, such formation increases the friction between cement particles and reduces the flow performance of cement particles. As a result, compressive strength of the cement decreases to invalidation. Therefore, the invalidation mechanism of Portland cement is the hydration reaction due to the absorption of moisture in the environment during storage. The hydration reaction degree increases with storage time, resulting in cement invalidation. The degree of the hydration reaction of potassium gypsum and the ettringite generated from the hydration reaction of oxides containing K and Al determine the invalidation degree.

As shown in Table 2, the content of oxide containing K of cement samples used in this paper was only 0.13%, meanwhile, the content of oxide containing K in most Portland cement in the whole world is very little and it could be basically unchanged within different periods under different relative humidity conditions. The content of oxide containing K was always little, and the change range was less than 1%, which indicated that the amount of potassium gypsum was minimal in the cement hydration, that is, potassium gypsum was not the main factor that caused cement invalidation. The content of oxide containing Al in the initial cement was 4.11%. Under different relative humidity conditions and storage periods, the contents of oxide containing Al in the area which indicated microstructure changes in SEM images changed significantly. The contents of oxide containing Al in the A7 to A90 samples increased from 3.3% to 15.5%, and the colour of the cement powder changed. Acicular crystals and agglomeration were evident when the content of oxide containing Al reached 12.6%. Meanwhile, the compressive strength of cement significantly decreased and approached complete invalidation. Acicular crystals were also apparent in the BSE images of samples B7 to B90, when the Al-containing oxide content increased from 3.5% to 6.9%. This increase in Al content was accompanied by mild agglomeration in the cement. At this time, the cement was invalid, and the agglomeration was remarkable in the cement when the Al-containing oxide content reached 15.7%. As shown in the BSE images, the acicular crystals formed a compact structure when the Al-containing oxide content reached 17.7%, and severe agglomeration occurred in the cement. The samples of C7 to C90 were also consistent. Therefore, cement invalidation in the experiments can be mainly attributed to the acicular crystals of Al-containing oxides, and the acicular crystals shown in the BSE images were mainly produced by the hydration reaction of Al-containing oxides.

### 3.2.2. Quantitative characterization

A quantitative invalidation characterization system of Portland cement was established based on the above test results and invalidation mechanism analysis. SEM observation samples were prepared to obtain BSE and EDS images. The following criteria were included in the characterization system. (1) If microscopic structures with acicular morphologies and lengths greater than 3.0  $\mu\text{m}$  are observed near the cement particles in the BSE images, the cement can be quantitatively judged to have undergone complete invalidation. (2) If the content of oxide containing Al in the area of ettringite formation is not more than 5.0%, then the cement does not exhibit invalidation. If the content of oxide containing Al in the area of ettringite formation exceeds 5.0%, then the invalidation has begun to occur. If the content of oxide containing Al in the area of ettringite formation exceeds 10.0%, then the cement can be judged quantitatively as exhibiting completely invalidation. The

method of quantitative invalidation characterization system of P-II 52.5 Portland cement is convenient compared to some existing methods such as visual observation and strength test method. The invalidation characterization system reduces required time and cost in actual application, meanwhile, it can accurately judge the invalidation degree of Portland cement.

### 3.3. Experimental verification

Four samples were collected from A1 to A4 stored in an environment with NaCl solution. The compressive strengths of the six 28-day cement mortar specimens in each group were tested [13]. Bleeding rate of sample labelled as A7 was normal and bleeding rate of sample A14 remained unchanged. However, bleeding rate of sample A30 increased slightly compared with sample A7 and sample A14. At the same time, water film on the surface of cement mortar could be observed clearly. With the increase of curing time, bleeding rate of sample A90 increased significantly. Meanwhile, thickness of water film on the surface of sample A90 increased than that of sample A30. In summary, bleeding rate of cement mortar increased with the degree of invalidation of cement.

The experimental results are shown in Table 6. In the BSE images of A7, no acicular structures longer than 3  $\mu\text{m}$  were observed, and the content of oxide containing Al was 3.3%, which did not exceed 5.0%. The invalidation characterization system proposed in this study revealed that the cement was not invalidated. The compressive strength of the 28-day cured cement mortar specimen was 53.2 MPa, which was greater than the specified 52.5 MPa. These results indicated that the cement mortar specimens were not invalidated, and the invalidation characterization was correct.

No acicular structures with lengths greater than 3.0  $\mu\text{m}$  were apparent in the BSE images of A14, and the content of oxide containing Al was 4.9%, which did not exceed but was close to 5.0%. Thus, non-invalidation could be inferred based on the invalidation characterization system. The measured compressive strength of the 28-day cured mortar specimen was 52.6 MPa, which is greater than 52.5 MPa in the standard requirement but less than the compressive strength of the mortar specimen from A7. These results suggested that the A14 cement was almost invalidated. The invalidation characterization was correct.

No acicular structures with lengths greater than 3.0  $\mu\text{m}$  were found in the BSE images of A30, but the content of oxide containing Al was 12.6%, which exceeded 10.0%. Thus, complete invalidation could be inferred by using the invalidation characterization system. The measured compressive strength of the 28-day cured cement mortar specimen was 47.3 MPa, which was 5.0 MPa lower than the value of 52.5 MPa in the standard requirement. This result suggested that A30 cement exhibited complete invalidation. The invalidation characterization was verified.

Acicular structures with lengths greater than 3.0  $\mu\text{m}$  were evident in the BSE images of A90, and the content of oxide containing Al was 15.5%, which exceeded 10.0%. The invalidation characterization system indicated complete invalidation. The measured compressive strength of the 28-day cured cement mortar specimen was 43.7 MPa, which was by over 5.0 MPa lower than the value of 52.5 MPa in the standard requirement. Thus, A90 cement exhibited complete invalidation. This result confirmed the invalidation characterization.

Some properties of Portland cement such as specific surface and its chemical composition exactly affect the invalidation of different type of Portland cement according to current research status. Therefore, a method of research on one type of Portland cement has been established in this paper. Related work will be carried out in the further study.

**Table 6**  
28 day compressive strength of mortar test values (MPa).

Test number	Sample label			
	A7	A14	A30	A90
1	54.4	52.3	47.1	44.7
2	51.9	51.7	48.5	44.4
3	53.3	53.3	47.7	43.5
4	54.4	54.2	46.8	42.8
5	52.0	52.2	46.5	43.4
6	53.2	52.0	47.2	44.2
Average compressive strength	53.2	52.6	47.3	43.7

#### 4. Conclusion

For P-II 52.5 Portland cement used in this paper, the main findings obtained in this study are summarized below:

- (1) The crystallisation corrosion occurred during hydration of C3A is the main cause of invalidation of cement, and the degree of invalidation of Portland cement can be quantitatively assessed by BSE/EDS analysis.
- (2) While the acicular microscopic crystal structures whose length over 3.0  $\mu\text{m}$  appear around the cement particles in the BSE images, the cement can be quantitatively judged as complete invalidation.
- (3) If the content of oxide containing Al in the area of ettringite formation is less than 5.0%, the cement can be judged to be not invalidated; if the content of oxide containing Al in the area of ettringite formation exceeds 5%, the cement begin to invalid; if the content of oxide containing Al in the area of ettringite formation exceeds 10%, the cement can be quantitatively judged as complete invalidation.

#### Acknowledgements

The authors gratefully acknowledge the financial supports from the National Key Research and Development Program of China under Grant No. 2017YFC0404902, National Natural Science Foundation of China under Grant No. 51309090, the Fundamental Research Funds for the Central Universities under Grant No. 2015B11814, Postgraduate Research & Practice Innovation Program of Jiangsu Province under Grant KYCX17\_0474, and State Key Laboratory for GeoMechanics and Deep Underground Engineering, China University of Mining & Technology under Grant No. SKLGDUEK1414.

#### References

- [1] C.L. Hu, Z.J. Li, Micromechanical investigation of Portland cement paste, *Constr. Build. Mater.* 71 (11) (2014) 44–52.
- [2] D. Nagrockiene, I. Pundiene, A. Kicaite, The effect of cement type and plasticizer addition on concrete properties, *Constr. Build. Mater.* 45 (2013) 324–331, <https://doi.org/10.1016/j.conbuildmat.2013.03.076>.
- [3] C. Rößler, A. Eberhardt, H. Kucerova, B. Möser, Influence of hydration on the fluidity of normal Portland cement pastes, *Cem. Concr. Res.* 38 (2008) 897–906.
- [4] E.N. Bs 197–1, Cement – Part 1: Composition, Specifications and Conformity Criteria for Common Cements, British Standards Institution, London, United Kingdom, 2011.
- [5] Yang Jian-wei, Wang Qiang, Yan Pei-yu, et al., Influence of quality of cement on performance of concrete, *Concrete* 10 (2012) 71–73.
- [6] Lian Hui-zhen, Discussion on method for selecting mix proportion of concrete problems in design of mix proportion of concrete, *Concrete* 03 (2009) 1–5.
- [7] Lin Yong-quan, Influence of cement quality fluctuation on the performance of ready-mixed concrete, *Cement* 1 (2003) 20–25.
- [8] Chen Han-ming, Technical diagnosis and countermeasure of cement agglomerate quality problem, *Cement* 2 (1999) 14–16.
- [9] Zou Hua-bin, Analysis of EDS fingerprint spectra of mineral drug montmorillonite powder relying on dual index grade sequence individualized pattern recognition method and their quickly quality evaluation, *Spectrosc. Spectra. Anal.* 12 (2013) 3321–3325.
- [10] He Bin, Failure analysis on steel structure component for outdoor building of substation, *Heat Treat. Met.* 32 (2007) 365–368.
- [11] L. Greenspan, Humidity fixed points of binary saturated aqueous solution, *Res. Nat. Bur. Stand. (U.S.)* 81A (1971) 213–230.
- [12] L. Struble, P.E. Stutzman, Epoxy impregnation of hardened cement for microstructural characterization, *J. Mater. Sci. Lett.* 8 (1989) 632–634.
- [13] GB/T 17671-1999, Methods of Testing Cements—Determination of Strength, National Standards of the People's Republic of China.
- [14] P.K. Mehta, Effect of lime on hydration of pastes containing gypsum and calcium aluminate or calcium sulfoaluminate, *J. Am. Ceram. Soc.* 56 (6) (1973) 315–319 [ISSN 0002-7820].
- [15] M. Katsioti, N. Patsikas, P. Pipilikaki, N. Katsiotis, K. Mikedi, M. Chaniotakis, Delayed ettringite formation (DEF) in mortars of white cement, *Constr. Build. Mater.* 25 (2011) 900–905.
- [16] P.K. Mehta, Mechanism of expansion associated with ettringite formation, *Cem. Concr. Res.* 3 (1976) 1–6.
- [17] J. Pourchez, F. Valdivieso, P. Grosseau, et al., Kinetic modelling of the thermal decomposition of ettringite into metaettringite, *Cem. Concr. Res.* 36 (11) (2006) 2054–2060.